



## Object-based feature selection for crop classification using multi-temporal high-resolution imagery

Qian Song, Mingtao Xiang, Ciara Hovis, Qingbo Zhou, Miao Lu, Huajun Tang & Wenbin Wu

To cite this article: Qian Song, Mingtao Xiang, Ciara Hovis, Qingbo Zhou, Miao Lu, Huajun Tang & Wenbin Wu (2019) Object-based feature selection for crop classification using multi-temporal high-resolution imagery, International Journal of Remote Sensing, 40:5-6, 2053-2068, DOI: [10.1080/01431161.2018.1475779](https://doi.org/10.1080/01431161.2018.1475779)

To link to this article: <https://doi.org/10.1080/01431161.2018.1475779>



Published online: 05 Jul 2018.



Submit your article to this journal [↗](#)



Article views: 221



View related articles [↗](#)



View Crossmark data [↗](#)



Citing articles: 2 View citing articles [↗](#)



# Object-based feature selection for crop classification using multi-temporal high-resolution imagery

Qian Song<sup>a</sup>, Mingtao Xiang<sup>a</sup>, Ciara Hovis<sup>b</sup>, Qingbo Zhou<sup>a</sup>, Miao Lu<sup>a</sup>, Huajun Tang<sup>a</sup> and Wenbin Wu<sup>a</sup>

<sup>a</sup>Key Laboratory of Agricultural Remote Sensing (AGRIRS), Ministry of Agriculture/Institute of Agricultural Resources and Regional Planning, Chinese Academy of Agricultural Sciences, Beijing, China; <sup>b</sup>Center for System Integration and Sustainability, Michigan State University, East Lansing, MI, USA

## ABSTRACT



With high-resolution remote-sensing data, there are numerous possible features for object description, making the selection of optimal features a time-consuming and subjective process. While substantial efforts have been made to compare the utility of feature selection metrics, less attention has been paid to the efficiency of such in the context of object-based image analysis. In this study, the statistical measurement z-score was used to ensure compatibility with objects. We assessed the feasibility of a z-score method, and then ranked and reduced input features using a backward elimination technique. The results showed that separability can be efficiently estimated based on z-score values, and the near-infrared band performed the best for crop classification. A straightforward trend was observed, and the optimal feature set was created, which was a combination of spectral, temporal, texture information and vegetation indices. These features complement one another to help increase crop map accuracy. For the 40% of the entire sample sizes, the optimal feature sets produced the best trade-off between the number of inputs and classification accuracy, with the misclassification error of 7.09%. Additionally, reliable crop maps were obtained, with the overall accuracy of 92.64%, and the z-score method showed great potential for the separability of crops at object scale using remotely sensed multi-temporal data.

## ARTICLE HISTORY

Received 30 November 2017  
Accepted 1 May 2018

## 1. Introduction

Having an accurate and reliable understanding of the distribution of crop types is critical for both decision-making and monitoring applications, e.g. crop acreage estimation, yield forecasting, growth monitoring, and hazard prediction (Belgiu and Csillik 2018; Mkhabela et al. 2011). Remote sensing plays an important role in obtaining crop spatial distribution information from regional to global scales due to its spatially explicit representation as well as its frequent temporal coverage (Pan et al. 2012; Song et al. 2017). Currently, with the development of remote sensing, high-resolution imagery has begun to be widely used

**CONTACT** Wenbin Wu  [wuwenbin@caas.cn](mailto:wuwenbin@caas.cn)  Key Laboratory of Agricultural Remote Sensing (AGRIRS), Ministry of Agriculture/Institute of Agricultural Resources and Regional Planning, Chinese Academy of Agricultural Sciences, Beijing, China

for crop mapping (Han et al. 2014; Singha, Wu, and Zhang 2017; Vieira et al. 2012). The traditional pixel-based classification method focused only on the spectral characteristics of high-resolution satellite images, therefore being unable to incorporate size, shape, texture, pattern, and contextual information (Peña et al. 2014; Zhang et al. 2017). Alternatively, object-based image analysis (OBIA) considers the spatial location and context of homogeneous pixels, allowing for crop type classification and crop growth monitoring at object level (Duro, Franklin, and Dub 2012). OBIA can extract meaningful image objects by segmentation and generate texture and spatial features in addition to spectral information. A wide range of information at the object level can help to increase the capacity of crop identification.

Many studies reveal that remote-sensing data can provide a diversity of multi-temporal, spectral and spatial features that well describe phenological changes of crops, many of which have been widely used for crop mapping activities (Costa et al. 2014; Hu et al. 2017; Mulianga et al. 2015). The crop growth stage, canopy structure, planting patterns, and soil background not only correspond to the reflectance signal captured by the sensor but also relate to the derived vegetation indices (Peña-Barragán et al. 2011). Most crop classifications methods focus on either the complete image spectral resolution of a time series or different vegetation index temporal profiles, e.g. normalized difference vegetation index (NDVI) and enhanced vegetation index (Peña and Brenning 2015). Apart from multi-spectral time series data, texture features have been used to define the structural and contextual attributes of every crop at a parcel scale and enrich the information available for crop mapping and monitoring (Patil and Lalitha 2012). These features are based either on spectral properties of crops and their canopy or on textural properties of the crop structure or in a combination where both are of particular interest. However, the availability of hundreds of multi-temporal multiple bands and their derivations as well as spatial-temporal features can make the determination of optimal features a time consuming or subjective process. Thus, knowing how to optimally use this wealth of information is crucial.

To address the problems associated with large volumes of features, various feature selection methods involving separation distances for image classes have been investigated. The well-known Jeffries–Matusita (JM) distance has been widely used to measure the separability of crops (Hao et al. 2015; Murakami et al. 2001). The median Mahalanobis distance, as a statistical separability criterion, is utilized to highlight the individual and combined influence of spectral and temporal features in land-cover classification (Carrao, Goncalves, and Caetano 2008). Besides those mathematical distance metrics, graphical methods and different embedded approaches such as the feature importance within Random Forest involve separation distances for image classes (Gao et al. 2015; Johansen and Phinn 2009). Given the large number of possible features for object description, substantial efforts have been made to compare the utility of feature selection metrics. However, less feature selection methods have been used in conjunction with OBIA.

To address this knowledge gap, the objective of this study uses a statistical measurement of z-score to (1) estimate the separability of spatio-temporal features based on Gaofen-1 temporal data at object level; (2) characterize the relatively small field size of the crops to find optimal combinations of feature sets and training sample sizes to classify the crop types of interest. We first determined the potential of each object-based

feature for crop mapping. Then the classification performance of each feature set was evaluated. We evaluated the stability of optimal feature sets when different training sample sets are used. Finally, we assessed the accuracy of crop mapping based on the optimal feature and training sample sets using the machine-learning Support Vector Machine (SVM).

## 2. Study area and data sets

### 2.1. Study area

Beian City is located approximately between 47°32'24" N and 48°34'12" N latitude and 126°15'36" E and 127°30'00" E longitude in northeast China (Figure 1). It has a long and frigid winter and a short and cool summer, with an average annual temperature of  $-0.6^{\circ}\text{C}$  to  $2.7^{\circ}\text{C}$  decreasing from southeast to northwest. Its annual average precipitation ranges from 500 to 700 mm, which is mostly concentrated in summer. Beian City is one of the most important production regions in northeast China. Nicknamed as the 'Window for government decision-making', this subarctic city is regarded as the key monitoring area for adjustment of crop planting structure. Its main crops include soybeans and corn, with little rice and wheat, all of which are harvested once each year due to the limited hours of sunshine and accumulated heat. Each crop has a well-defined crop calendar and unique seasonal growth pattern. For instance, soybean in Beian City is generally sowed in mid-May to late May, proceeding emergence, three leaves, seven leaves, blooming, bearing pod, filling seed, senescence, and harvested in late-September. The crop calendar for corn is from late April to end of September, and for wheat it is from early April to late July. Rice is transplanted in early June and harvested in late September, experiencing a relatively long growing period.

### 2.2. Data collection and processing

Launched on 26 April 2013, the Gaofen-1 satellite (GF-1) represents the first optical satellite of the 'Chinese high-resolution satellite' programme. The GF-1 satellite carries four medium spatial resolution wide field-of-view (WFV) cameras. The multispectral images obtained from GF-1 WFV sensor has coverage of 450–890 nm and four optical bands (i.e. blue, green, red, and near-infrared) at a 16 m resolution. The specification of GF-1 WFV sensor is listed in Table 1.

Spring wheat is planted earliest in April, and most crops are harvested in late September. Thus, we selected four scenes of cloud-free GF-1 WFV data ranging from no crop cover stage to crop harvest stage (Table 2). The data were downloaded from the China Centre for Resource Satellite Data and Application (<http://www.cresda.com/CN/>). Radiometric calibration using the calibration coefficient provided by CCTSDA was performed for all the GF-1 WFV image pixels. Atmospheric corrections using Fast Line-of-sight Atmospheric Analysis of Spectral Hypercubes module were implemented. The ortho-rectification based on the rational polynomial coefficient file in system was also performed in ENVI as well. All high-quality imageries were georeferenced to UTM WGS84 (zone 52N-WGS84) projection system using the pan band of Landsat-8 images acquired on 24 September 2014 in Beian.

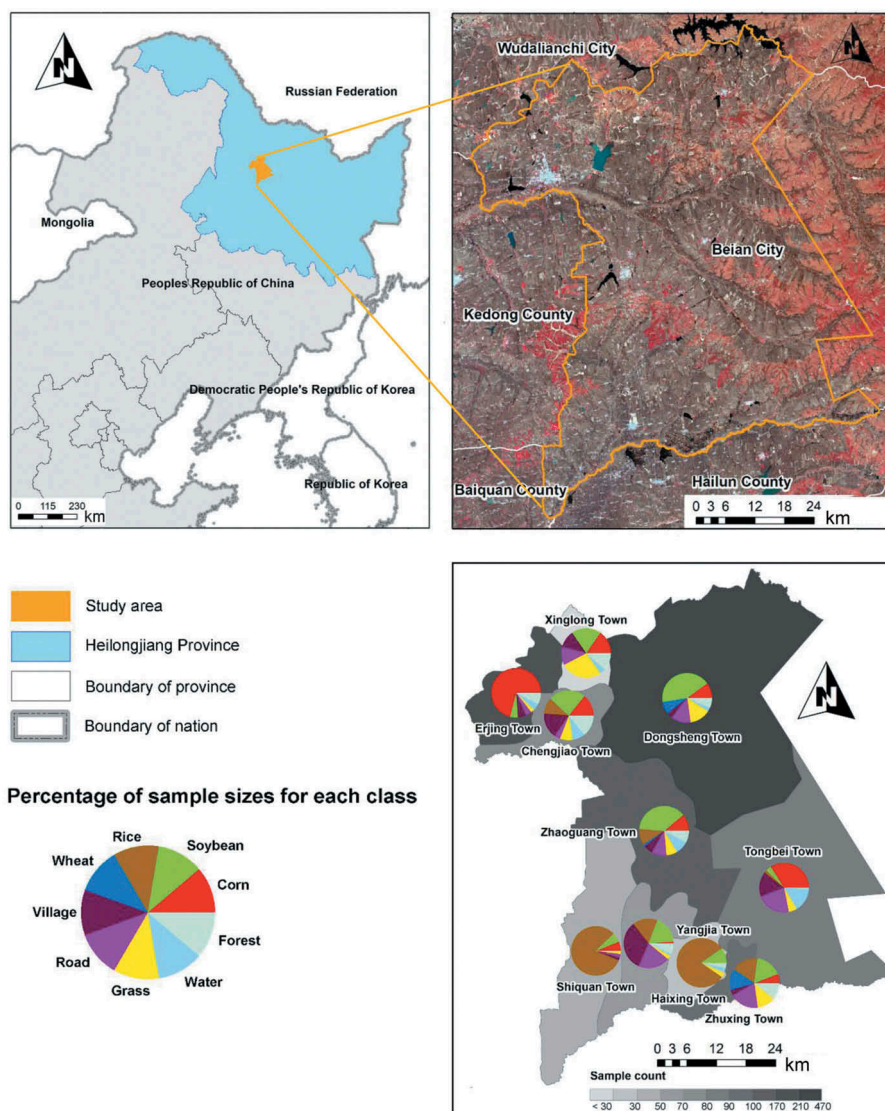


**Figure 1.** The geolocation of study area, with the Gaofen Satellite no. 1 wide field-of-view cameras (GF-1 WFV) 16 m false colour image (R = near-infrared, G = Red, B = G) acquired on 24 April 2014.

**Table 1.** Specification of GF-1 WFV sensor.

Satellite	Sensor	Bands	Wavelength range (nm)	Spatial resolution (m)	Swath width (km)	Repeat cycle (day)
GF-1	WFV	1 (Blue)	450–520	16	800 (four cameras combined)	4
		2 (Green)	520–590			
		3 (Red)	630–690			
		4 (near-infrared)	770–890			

**Table 2.** Data sets used in the study.

Satellite	Sensor	Acquisition date	Crop developing status
GF-1	WV1	24 April 2014	No crop cover
GF-1	WV3	24 May 2014	Green-up
GF-1	WV3	25 July 2014	Maturity
GF-1	WV2	24 September 2014	Senescence

### 2.3. Field sample data

To assess the performance of crop classification, an extensive field survey was carried out in summer. In this study, a distance of no less than 1 km was chosen as the sampling interval collecting 1777 sampling points. We collected 1121 crop (corn, soybean, rice, and wheat) samples and 626 non-crop classes (mainly village, road, water, forest, and grassland) samples through field surveys. Only a field with area greater than 256 m<sup>2</sup> (16 m × 16 m) was selected as the sample plot. We created those plots over the available fine resolution GF-1 WV images. In addition to training samples, a total of 530 points were kept aside for validation.

## 3. Methodology

### 3.1. Segmentation of multi-temporal GF-1 WV images

GF-1 WV images were segmented into homogeneous objects using one of the most popular multi-resolution segmentation (MRS) algorithms for OBIA in eCognition Developer 8.7. MRS algorithm uses a bottom-up region merging technique that starts from the pixel level and iteratively aggregates pixels into objects. Spatially adjacent segments are merged based on the degree of heterogeneity that is largely defined by the scale parameter. To avoid time-consuming trial-and-error and subjective selection of the scale parameter, Estimation of Scale Parameter 2 (ESP2) was used for assisting the segmentation to dictate the size and homogeneity of the resultant objects in an automated way (Drăguț et al. 2014). The fundamental idea of ESP2 is to select the segmentation scales based on the rate of change for the calculated local variance of object heterogeneity at various scales. The scales corresponding to the peaks of the rate of change were deemed as the appropriate segmentation parameters. The two mutually exclusive parameters, i.e. colour and shape, determined the relative weighting of reflectance and shape. The shape is composed of smoothness and compactness properties and the total weighted value of smoothness and compactness equals one.

We used the blue, green, red, and near-infrared spectral bands of four GF-1 images in the segmentation process. All multi-temporal bands were weighted equally for the segmentation. A hierarchical segmentation approach was implemented in ESP2. Based on a three-level hierarchy concept, we implemented an automated image segmentation process at three default scale increments of 1, 10, and 100, with the start scale of 1 at each level. The weights of colour and shape were set to 0.9 and 0.1, respectively. The weights of smoothness and compactness were set to 0.5 and 0.5, respectively. After setting the algorithm parameters of ESP2, the rate of change for the local variance was calculated and then a scale parameter of 30 were selected as the potential scales which corresponds to local maximum, resulting in 119,660 objects.

### 3.2. z-Score for feature selection

The MRS approach provides the possibility of evaluating new spectral, textural, and spatial features at the object level. Canopy structure, leaf pigment, leaf water, planting patterns, and soil background not only highly relate to the reflectance signal captured by the sensor and the derived vegetation indices but also define the spatial structural and textural attributes of every crop at the field scale (Drăguț et al. 2014). Thus, we calculated a set of 166 object features, which were categorized in three groups (Table 3): (1) object spectral information based on mean and standard deviation (SD) values as well as vegetation indices, (2) object textural information based upon the grey-level co-occurrence matrix (GLCM), and (3) object spatial information based on shape or colour.

The essence of crop classification is to minimize the spectral variability within ( $\Delta_{intra}$ ) and maximize the spectral difference between ( $\Delta_{inter}$ ) pairwise comparisons of crops. Previous studies proposed separability metrics based on statistical theory. These pairwise separability metrics are used to detect the spectral variability within ( $\Delta_{intra}$ ) and between ( $\Delta_{inter}$ ) species, which was already used to evaluate the spectro-temporal separability and to select the optimal features for classification (Somers and Asner 2013).

Compared with the well-known JM distance, a statistical measurement of z-score is more compatible with eCognition's exported objects. Furthermore, similarly to the widely used separability index (Hu et al. 2016), the z-score is a pairwise measure of class separability based on the probability distributions of two classes and is calculated as (Kreyszig 1979):

$$z\text{-score} = \frac{\Delta_{inter}(i,j)}{\Delta_{intra}(i,j)} = \frac{|\bar{X}_i - \bar{X}_j|}{\sqrt{\frac{\sigma_i^2}{n_i} + \frac{\sigma_j^2}{n_j}}} \quad (1)$$

where  $\bar{X}_i$  and  $\bar{X}_j$  are the mean variable values for land-cover class  $i$  and class  $j$ , respectively, and  $\sigma_i$  and  $\sigma_j$  are the SD of classes  $i$  and  $j$ , respectively.  $n_i$  and  $n_j$  represent the sample sizes for classes  $i$  and  $j$ .  $|\bar{X}_i - \bar{X}_j|$  reflects the interclass variability. Given different weights to account for the different sample sizes of each class,  $\sqrt{\sigma_i^2/n_i + \sigma_j^2/n_j}$

**Table 3.** Description of features used in this study.

Category/name	Layers for each pairwise
Object spectral	
Mean (blue, green, red and near-infrared)	4 bands × 4 dates
Vegetation indices (RI, RVI,NDVI,EVI)	4 VIs × 4 dates
Standard deviation	4 bands × 4 dates
Object texture	
GLCM entropy	4 bands × 4 dates
GLCM correlation	4 bands × 4 dates
GLCM dissimilarity	4 bands × 4 dates
Object spatial	
Brightness	1
Compactness	1
Shape index	1
Length-width ratio	1
Rectangle	1
Density	1

RI, red vegetation index; RVI, ratio vegetation index; NDVI, normalized difference vegetation index; EVI, enhanced vegetation index; VIs, vegetation indices.



represents the intraclass variability. Thus, based on the input sample data, we can test the z-score, and a separability for each pairwise crop class is estimated based on the means and variances of the two crop classes in question.

### **3.3. SVM classification and accuracy assessment**

All features were then classified using the SVM classifier. SVM is a non-parametric classification approach that is based on a structural risk-minimization strategy and exploits a margin-based criterion (Pal and Foody 2010). Given the ability of handling nonlinear separation boundaries, generalizing well from a limited number of training samples, and supporting high-dimensional feature inputs, SVM outperforms other classifiers, such as the Maximum Likelihood Classifier, artificial neural networks, and Random Forests, when addressing various purposes including land use/crop mapping (Alganci et al. 2013; Mountrakis et al. 2011). For non-linearly separable input spaces, a kernel function is employed to transform the training data into a higher-dimensional feature space. In this study, the widely used radial basis function (RBF) kernel was selected for this analysis. The RBF kernel relies on two crucial parameters that need to be tuned. These include the gamma parameter ( $G$ ) and the regularization cost parameter ( $C$ ), which determine the width of the kernel and the penalty associated with misclassified training samples, respectively (Huang, Davis, and Townshend 2002). The  $G$  and  $C$  parameters were tuned by the function of 'tune.svm' with a grid search method in the package 'e1071' of R Programming Language. The optimization iterates through a 10-fold cross-validation, with the values of the  $G$  and  $C$  parameters ranging from  $10^{-2}$  to  $10^2$ . The parameters were ultimately set as 0.01 for  $G$  and 10 for  $C$  for feature sets.

According to the z-score value, backward feature selection was performed for the best-performing SVM classifier in order to determine how to achieve comparable results with a reduced number of features. Only when the accuracy of crop map was higher than the threshold value, the backward elimination was carried out. The threshold value should be set to be far below the expected accuracy (great than 85%). In this study, we set the threshold value as 55%.

The tuned SVM was used to generate the crop classification map of the studied area. For the classification map, we used 530 sample points for the accuracy assessment. The confusion matrix method was applied to measure accuracy of the resulting classification. The accuracy of crop classification was evaluated in terms of overall accuracy, producer's accuracy (PA), user's accuracy (UA), and kappa coefficient ( $\kappa$ ).

## **4. Results**

### **4.1. The potential of each object-based feature for crop mapping**

Figure 2 presented the z-score chart of each multi-temporal spectral and texture feature for the pairwise crop classes. As the z-score value increases, the crop pairwise classes for a given vegetation index became more separable, and the corresponding grid in the chart becomes increasingly red. A z-score of 35.7 was observed for the 'crop-soybean' class, representing the highest separability for this specific pairwise responding to near-infrared band in autumn. We observed more consistency in the change tendency of z-score values among corn, soybean, and rice than between wheat and the other three





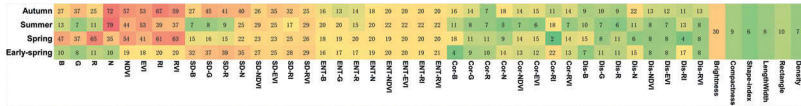


Figure 3. z-score charts for multiple crops with the sum of each pairwise class.

remaining features (Figure 4). Each variable of the GF-1 data contributes to the improved map accuracy. The trend is straightforward, although some of the variables contribute relatively little. When all of the features were taken as input data, the overall classification accuracy of 90.70% was first observed. The feature scenario (FS) corresponding to all the input features was devised as FS1. The acceptable accuracy of FS1 showed the strong ability of SVM in classifying a huge of number of variables without feature selection, even though some of which may be highly correlated. Two special points were also of interest: one providing for the highest accuracy (corresponding to FS2) and the other one providing for the biggest acceptable accuracy decrease (corresponding to FS3) when backward elimination performing. Note that the overall accuracy achieved to 92.45% by using only 40 remaining variables in FS2. This optimal accuracy in FS2 was higher than FS1, as those features effectively preserved the dynamic seasonal characteristics of the crops. The overall performance achieves acceptable accuracies with the overall classification accuracy of 91.35% before removing the SD of green band obtained during the crop senescence stage due to the relatively small noise influence. The largest variation of accuracy arrives at 1.15% when there are only 13 variables left. Additionally, the accuracy sharply dropped from 87.98% to 83.16% when the RVI from the green-up GF-1 image was

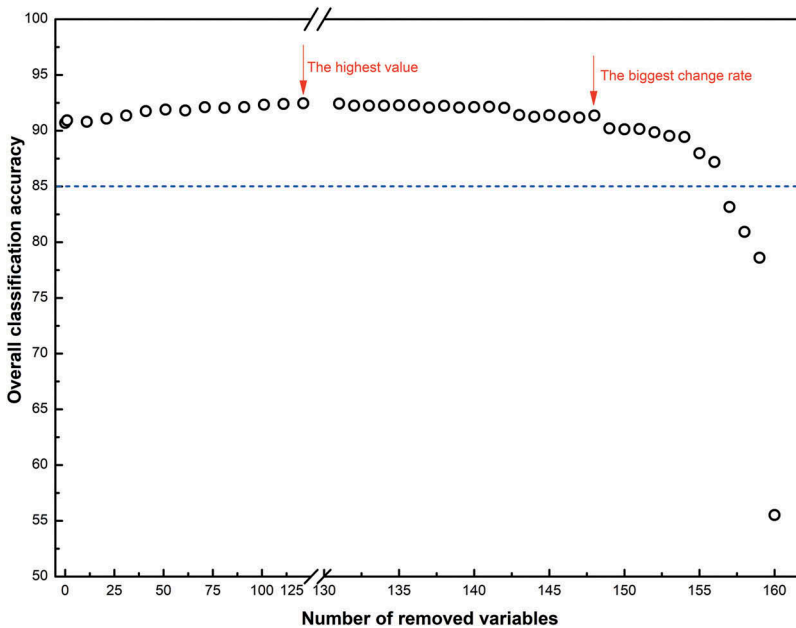


Figure 4. Overall classification accuracies based on backward elimination of the least z-score variable.

removed, due to the fact that it is the time when wheat and the other crops showed the greatest difference. Only features with a z-score value greater than 63 were retained, ensuring the expected 85.00% of overall accuracy can be obtained. The optimal variables for the key points marked in [Figure 4](#) are listed in [Table 4](#).

It is easily concluded that all of features used in the classification failed to provide meaningful information to improve crop classification accuracy. Although SVM was originally designed for supporting high-dimensional feature inputs, both noise from misregistration of the multi-temporal GF-1 data and high correlations between the features undermined crop map accuracy when substantial features were taken as input data. Therefore, feature selection reduced the computation and at the same time can efficiently search for an improved the classification accuracy.

### 4.3. The performance of different sample sizes

The effects of the number of training data on classification accuracy were evaluated using the misclassification error rate (MER) ([Figure 5](#)). MER differences of the feature sets ranged from 0.08% to 11.76% and varied with the training sample size. When the number of training samples was between 10% and 30% of the entire sample size, the MERs obtained with FS1 and FS3 changed significantly. When the training sample size was 40% or 70% of the entire sample size, classification performances obtained with FS1 and FS3 were almost identical. FS1 provided relatively higher MER across the 10 training sample sizes than classifications using FS2, except for a total of 40% sample points selected. FS1 started with poorer classification performances for smaller training sample sizes but had similar results as FS3 when using the 50% of training sample size. This indicated that the inclusion of more features may lead to reduced map accuracy due to a limited number of training samples. As expected, with the sample size increasing, the MRE for FS3 sustained declined ranging from 13.97% to 8.59%. FS2 balanced the computational cost and classification accuracy when larger than 80% of samples were taken as input data with the MER difference not significantly changing. The slight change of MER was attributed to reducing the risk of impacting by some atypical samples. Thus, FS2 was almost the best-performing feature set at each of the training sample sizes, providing the minimum MER at all 1777 field plots (MER < 11.15%). When 40% of samples were input into SVM with FS2, the lowest MER of 7.09% was obtained.

**Table 4.** Groups of the optimal variables for crop classification.

Feature scenario	Variables	Number of feature set
FS1:all	All features	166
FS2:the highest	N7, N9, RI9, R5, RV15, RI5, RV19, NDVI9, NDVI5, EVI7, EVI9, B5, SD-G9, NDVI7, SD-R9, EVI5, SD-N9, SD-R4, RI7, G5, RV17, G9, SD-G4, SD-N4, N5, SD-EVI9, SD-B4, SD-RI9, Brightness, SD-RV14, SD-RV17, SD-NDVI7, SD-RI4, SD-B9, SD-NDVI4, B9, SD-RV15, SD-NDVI9, R9, SD-RV19	40
FS3:the biggest change	N7, N9, RI9, R5, RV15, RI5, RV19, NDVI9, NDVI5, EVI7, EVI9, B5, SD-G9	13

Feature components: blue spectral band (B); green spectral band (G); red spectral band (R); near-infrared spectral band (N); red vegetation index (RI); ratio vegetation index (RVI); normalized difference vegetation index (NDVI); enhanced vegetation index (EVI); standard deviation of mean spectral feature (SD); extracted from the images acquired in April (4); extracted from the images acquired in May (5); extracted from the images acquired in July (7); extracted from the images acquired in September (9).

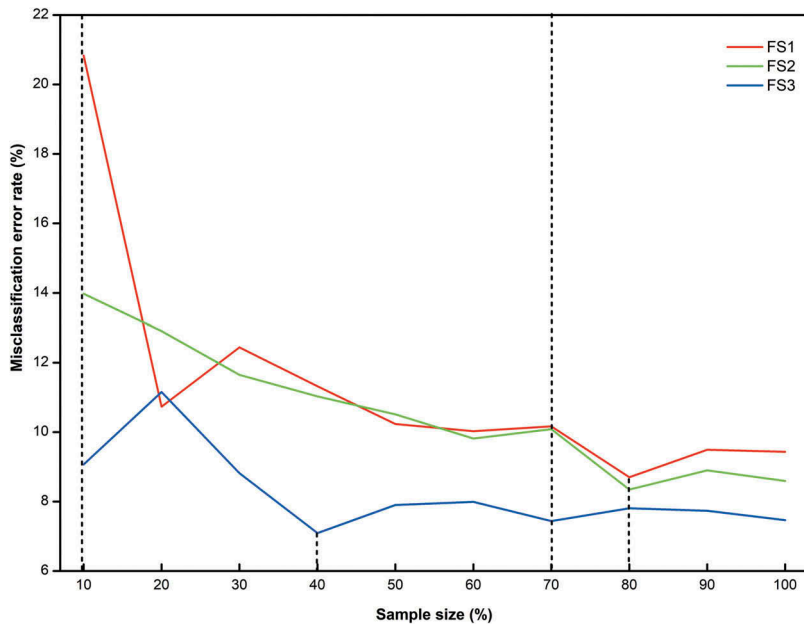


Figure 5. Cross-validated MERs for crops using different training sample size.

#### 4.4. Crop classification accuracy

The classifications of crop distribution using three different features and training sample size were performed: the combination of FS1 and 80% of the entire training samples represented the case of employing vast features and a huge number of training samples for crop identification; the combination of FS3 and 80% of the entire training samples represented the case where few features but a huge number of training samples for crop identification; the combination of FS2 and 40% of the entire training samples represented the case where few features and small training samples for crop identification. The classification accuracies of each class, including PA and UA, are shown in Table 5. We found the basic pattern of the PA and UA for each class was very similar. Using all the input available provided by GF-1 WFV, and field samples, the map accuracy was 90.85%. Compared with better classification from feature reduction, the 0.84% map accuracy increase is small. Feature reduction was particularly helpful in wheat class classification when combined with sufficient training sample data. Doing so resulted in a PA of wheat higher than 70%. Except for rice and wheat, the PA and UA for corn, soybean, and other classes all increased approximately 0.50–5.04% when features and training samples were optimized compared to a redundant input.

The crop classification map using the 40% of the training samples based on the optimal temporal spectral and spatial features corresponding to FS2 and SVM is shown in Figure 6. This is mapped with an overall accuracy of 92.64%, reaching a  $\kappa$  of 0.8948. Additionally, the backward feature selection strategy reduced the data redundancy and contributed to improved results. The user's accuracy, which is a measure of commission error and indicates the probability that a category classified on the map actually represents that category on the ground, ranged from 68.18% for wheat class to

**Table 5.** Accuracy for crop mapping based on different input data.

Feature scenario	FS1		FS2		FS3	
Sample size (%)	80		40		80	
Accuracy (%)	UA	PA	UA	PA	UA	PA
Corn	93.10	96.60	93.69	95.41	92.34	94.91
Soybean	93.09	93.31	95.59	94.20	92.20	93.39
Rice	72.12	96.15	79.25	97.67	86.27	92.63
Wheat	61.36	93.10	68.18	93.75	70.27	96.30
Others	97.09	85.87	96.15	89.29	94.20	88.64
Overall accuracy	90.85		92.64		91.69	
$\kappa$	0.8710		0.8948		0.8834	

96.15% for the other classes. User accuracies were excellent for corn and soybean (93.69% and 95.89%, respectively), but a completely mixed-free classification is unlikely with actual field boundaries. The lowest user's accuracy was attained for wheat, which occurred in a small cultivated area. The producer's accuracy of the individual categories, which is a measure of omission error and indicated the probability of actual spatial distribution being correctly classified, ranged from 89.29% for the others class to 97.67% for rice class. The producer accuracy for rice was excellent, but the user accuracy was only 79.25%. Therefore, the optimal input data applying for much finer spatial resolution may greatly enhance the accuracy.

## 5. Discussions

In this study, we used a statistical measurement of z-score for the selection of optimal features to classify crop types of interest at the object level and analyzed the influence of the number of features and training samples on crop identification. The desired accuracies were provided using optimal input data according to the z-score values. We determined that z-score measure was helpful for the object-based feature selection based on its ability to rank and reduce features, relatively low processing times, and relatively high accuracy. The backward elimination technique for multiple crop cultivation also indicates the strengths of the temporal GF-1 data for crop mapping as its high temporal and spatial resolutions effectively preserve the dynamic phenological characteristics of crops. Since huge temporal and spatial features of new 'both high' sensors are available at the global scale, there is great promise for crop mapping at regional scales when it combined with feature selection based on z-score.

Previous studies have shown that rather than using a large volume of spectral, temporal, and texture features, key features can achieve acceptable classification accuracy (Hao et al. 2015). The near-infrared band obtained the highest sum of all two-class z-score, which indicated that this feature can play an important role in improvement of classification accuracy. These results were consistent with the findings that the red and near-infrared bands were more effective for crop classification (Zhu et al. 2012). Additionally, spatial features, such as compactness, shape index, rectangle, or the ratio between lengths and widths, performed poorly, which is also consistent with the findings of Vieira et al. (2012), with classification accuracies less affected by the spatial features than spectral or texture features. More importantly, the improvement of classification accuracy is straightforward when backward elimination technique is employed as it iteratively removes features that do not contribute much to the classification.

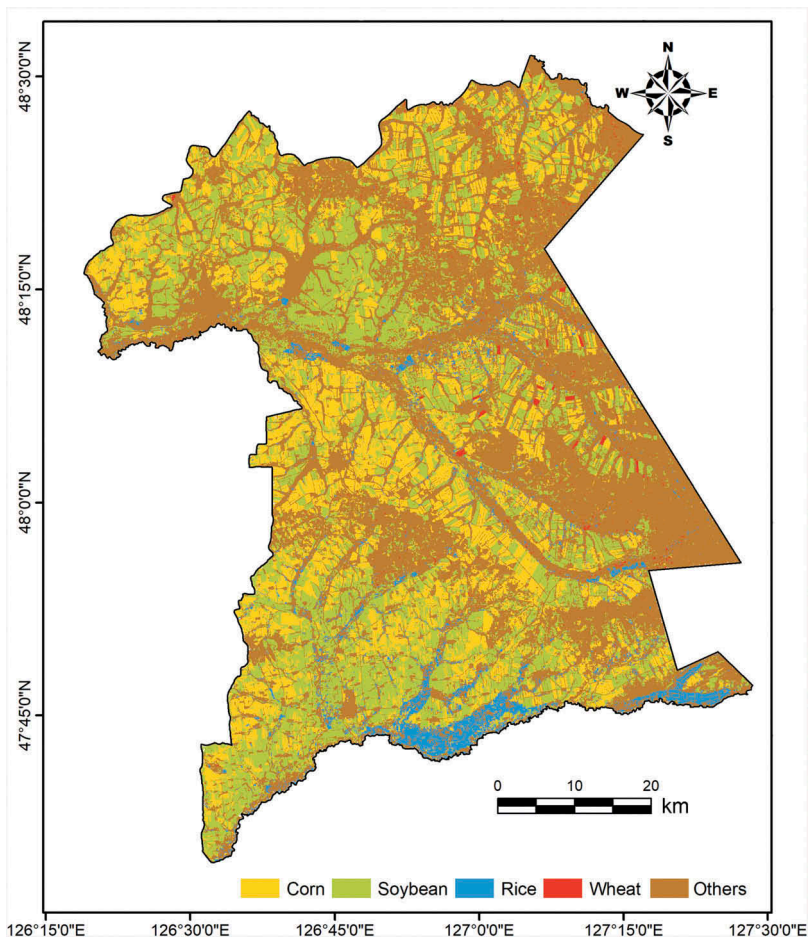


**Figure 6.** Classification map of multiple crops based on FS2 with 40% of training sample size.

The z-score method has the advantage of quantitative pairwise crop class separability. It has proven to be an excellent feature reduction and ranking tool. Additionally, the results were easy to interpret. This criterion required few steps and was easily compatible with object-based export. However, the z-score method has the disadvantage of not being robustly scaled, which makes it inconvenient for comparing separability of the same classes in different plots. We also acknowledge that the z-score criterion provides values for separating only two classes. We suggest that z-score criterion is appropriate if class separation distances are of interest, and if the analyst desires to rank input features for two-class comparisons. In this study, we only tested SVM classification using different sizes of training samples. Subsequent work will compare z-score with the feature selection methods, such as JM, classification tree analysis, and feature space optimization to assess the suitability of a particular feature selection approach.



## 6. Conclusion

In this study, we presented and evaluated a method for mapping crop spatial distribution at 16 m spatial resolution using multi-temporal GF-1 WFV data. We developed a statistical measurement of z-score to estimate the feature contributions at the object level, focusing on Beian City of China in 2014. The contributions of spectral, temporal, and spatial features can be efficiently assessed to increase classification accuracies. Our analyses showed that the separability of near-infrared band estimated by z-score compares well with the common view but the z-score has the disadvantage of lacking of fixed scale, which makes it inconvenient for comparing separability of the same classes in different plots. The straightforward elimination results presented great potential of using ranked features based on z-score, and ensured that the crop classes in question are discriminated effectively and with sufficiently high accuracy. However, if the training sample size is too small (i.e. less than 40% of the entire training samples), atypical samples lead to unacceptable misclassification errors. Therefore, we performed the crop classification by combining the top 40 features and 40% of the entire training samples, and the desirable accuracy was 92.64%. Further studies will investigate the validity of these findings when the z-score metric is applied to classifications of larger areas based on a dense satellite image time series.

## Acknowledgment

The authors thank the fellows at the Remote Sensing Technology Center, Heilongjiang Academy of Agriculture Sciences, for supporting the essential field investigation and crop samples.

## Disclosure statement

No potential conflict of interest was reported by the authors.

## Funding

This research is supported by the Opening Foundation of Key Laboratory of Agricultural Remote Sensing, Ministry of Agriculture [2017004], by the National Key Research and Development Programme of China [2017YFE0104600], by the Chinese Academy of Engineering Consulting Project [2016-ZCQ-08], and by the Elite Youth Programme of Chinese Academy of Agricultural Sciences [CAASQNYC-KYPY-11].

## References

- Alganci, U., E. Sertel, M. Ozdogan, and C. Ormeci. 2013. "Parcel-Level Identification of Crop Types Using Different Classification Algorithms and Multi-Resolution Imagery in Southeastern Turkey." *Photogrammetric Engineering & Remote Sensing* 79 (11): 1053–1065. doi:10.14358/PERS.79.11.1053.
- Belgiu, M., and O. Csillik. 2018. "Sentinel-2 Cropland Mapping Using Pixel-Based and Object-Based Time-Weighted Dynamic Time Warping Analysis." *Remote Sensing of Environment* 204: 509–523. doi:10.1016/j.rse.2017.10.005.
- Carrao, H., P. Goncalves, and M. A. R. Caetano. 2008. "Contribution of Multispectral and Multitemporal Information from MODIS Images to Land Cover Classification." *Remote Sensing of Environment* 112 (3): 986–997. doi:10.1016/j.rse.2007.07.002.



- Costa, H., H. Carrão, F. Bação, and M. Caetano. 2014. "Combining Per-Pixel and Object-Based Classifications for Mapping Land Cover over Large Areas." *International Journal of Remote Sensing* 35 (2): 738–753. doi:10.1080/01431161.2013.873151.
- Drăguț, L., O. Csillik, C. Eisank, and D. Tiede. 2014. "ESP2: Automated Parameterisation for Multi-Scale Image Segmentation on Multiple Layers." *ISPRS Journal of Photogrammetry and Remote Sensing* 88: 119–127. doi:10.1016/j.isprsjprs.2013.11.018.
- Duro, D. C., S. E. Franklin, and E. M. G. Dub. 2012. "Multi-Scale Object-Based Image Analysis and Feature Selection of Multi-Sensor Earth Observation Imagery Using Random Forests." *International Journal of Remote Sensing* 33 (14): 4502–4526. doi:10.1080/01431161.2011.649864.
- Gao, T., J. Zhu, X. Zheng, G. Shang, L. Huang, and S. Wu. 2015. "Mapping Spatial Distribution of Larch Plantations from Multi-Seasonal Landsat-8 OLI Imagery and Multi-Scale Textures Using Random Forests." *Remote Sensing* 7 (2): 1702–1720. doi:10.3390/rs70201702.
- Han, N., H. Du, G. Zhou, X. Sun, H. Ge, and X. Xu. 2014. "Object-Based Classification Using SPOT-5 Imagery for Moso Bamboo Forest Mapping." *International Journal of Remote Sensing* 35 (3): 1126–1142. doi:10.1080/01431161.2013.875634.
- Hao, P., Y. Zhan, L. Wang, Z. Niu, and M. Shakir. 2015. "Feature Selection of Time Series MODIS Data for Early Crop Classification Using Random Forest: A Case Study in Kansas, USA." *Remote Sensing* 7 (5): 5347–5369. doi:10.3390/rs70505347.
- Hu, Q., W. Wu, Q. Song, M. Lu, D. Chen, Q. Yu, and H. Tang. 2017. "How Do Temporal and Spectral Features Matter in Crop Classification." *Journal of Integrative Agriculture* 16 (2): 324–336. doi:10.1016/S2095-3119(15)61321-1.
- Hu, Q., W. Wu, Q. Q. Yu, M. Lu, P. Yang, H. Tang, and Y. Long. 2016. "Extending the Pairwise Separability Index for Multicrop Identification Using Time-Series MODIS Images." *IEEE Transactions on Geoscience and Remote Sensing* 54 (11): 6349–6361. doi:10.1109/TGRS.2016.2581210.
- Huang, C., L. S. Davis, and J. R. G. Townshend. 2002. "An Assessment of Support Vector Machines for Land Cover Classification." *International Journal of Remote Sensing* 23 (4): 725–749. doi:10.1080/01431160110040323.
- Johansen, K., and S. Phinn. 2009. "Mapping Banana Plantations from Object-Oriented Classification of SPOT-5 Imagery." *Photogrammetric Engineering and Remote Sensing* 75 (9): 1069–1081. doi:10.14358/PERS.75.9.1069.
- Kreyszig, E. 1979. *Advanced Engineering Mathematics*. New York: John Wiley & Sons.
- Mkhabela, M., P. Bullock, S. Raj, S. Wang, and Y. Yang. 2011. "Crop Yield Forecasting on the Canadian Prairies Using MODIS NDVI Data." *Agricultural and Forest Meteorology* 151: 385–393. doi:10.1016/j.agrformet.2010.11.012.
- Mountrakis, G., J. Im, and C. Ogole. 2011. "Support Vector Machines in Remote Sensing: A Review." *ISPRS Journal Of Photogrammetry and Remote Sensing* 66 (3): 247–259.
- Mulianga, B., A. Bégué, P. Clouvel, and P. Todoroff. 2015. "Mapping Cropping Practices of a Sugarcane-Based Cropping System in Kenya Using Remote Sensing." *Remote Sensing* 7 (11): 14428–14444. doi:10.3390/rs71114428.
- Murakami, T., S. Ogawa, N. Ishitsuka, K. Kumagai, and G. Saito. 2001. "Crop Discrimination with Multitemporal SPOT/HRV Data in the Saga Plains, Japan." *International Journal of Remote Sensing* 22: 1335–1348. doi:10.1080/01431160151144378.
- Pal, M., and G. M. Foody. 2010. "Feature Selection for Classification of Hyperspectral Data by SVM." *IEEE Transactions on Geoscience and Remote Sensing* 45 (5): 2297–2307. doi:10.1109/TGRS.2009.2039484.
- Pan, Y., L. Li, J. Zhang, S. Liang, X. Zhu, and D. Sulla-Menashe. 2012. "Winter Wheat Area Estimate from MODIS-EVI Time Series Using the Crop Proportion Phenology Index." *Remote Sensing of Environment* 119: 232–242. doi:10.1016/j.rse.2011.10.011.
- Patil, A., and Y. S. Lalitha. 2012. "Classification of Crops Using FCM Segmentation and Texture, Colour Feature." *International Journal of Advanced Research in Computer and Communication Engineering* 1 (6): 371–377.
- Peña, J., P. Gutiérrez, C. Hervás-Martínez, J. Six, R. Plant, and F. López-Granados. 2014. "Object-Based Image Classification of Summer Crops with Machine Learning Methods." *Remote Sensing* 6 (6): 5019–5041. doi:10.3390/rs6065019.

- Peña, M. A., and A. Brenning. 2015. "Assessing Fruit-Tree Crop Classification from Landsat-8 Time Series for the Maipo Valley, Chile." *Remote Sensing of Environment* 171: 234–244. doi:[10.1016/j.rse.2015.10.029](https://doi.org/10.1016/j.rse.2015.10.029).
- Peña-Barragán, J. M., M. K. Ngugi, R. E. Plant, and J. Six. 2011. "Object-Based Crop Identification Using Multiple Vegetation Indices, Textural Features and Crop Phenology." *Remote Sensing of Environment* 115 (6): 1301–1316. doi:[10.1016/j.rse.2011.01.009](https://doi.org/10.1016/j.rse.2011.01.009).
- Singha, M., B. Wu, and M. Zhang. 2017. "Object-Based Paddy Rice Mapping Using HJ-1A/B Data and Temporal Features Extracted from Time Series MODIS NDVI Data." *Sensors* 17 (10): 1–17.
- Somers, B., and G. P. Asner. 2013. "Multi-Temporal Hyperspectral Mixture Analysis and Feature Selection for Invasive Species Mapping in Rainforests." *Remote Sensing of Environment* 136: 14–27. doi:[10.1016/j.rse.2013.04.006](https://doi.org/10.1016/j.rse.2013.04.006).
- Song, X., P. V. Potapov, A. Krylov, L. King, C. M. Di Bella, A. Hudson, A. Khan, B. Adusei, S. V. Stehman, and M. C. Hansen. 2017. "National-Scale Soybean Mapping and Area Estimation in the United States Using Medium Resolution Satellite Imagery and Field Survey." *Remote Sensing of Environment* 190: 383–395. doi:[10.1016/j.rse.2017.01.008](https://doi.org/10.1016/j.rse.2017.01.008).
- Vieira, M. A., A. R. Formaggio, C. D. Rennó, C. Atzberger, D. A. Aguiar, and M. P. Mello. 2012. "Object Based Image Analysis and Data Mining Applied to a Remotely Sensed Landsat Time-Series to Map Sugarcane over Large Areas." *Remote Sensing of Environment* 123: 553–562. doi:[10.1016/j.rse.2012.04.011](https://doi.org/10.1016/j.rse.2012.04.011).
- Zhang, H., Q. Li, J. Liu, X. Du, T. Dong, H. McNairn, C. Champagne, M. X. Liu, and J. L. Shang. 2017. "Object-Based Crop Classification Using Multi-Temporal SPOT-5 Imagery and Textural Features with a Random Forest Classifier." *Geocarto International* 32: 1–19. doi:[10.1080/10106049.2017.1333533](https://doi.org/10.1080/10106049.2017.1333533).
- Zhu, Z., C. E. Woodcock, J. Rogan, and J. Kellndorfer. 2012. "Assessment of Spectral, Polarimetric, Temporal, and Spatial Dimensions for Urban and Peri-Urban Land Cover Classification Using Landsat and SAR Data." *Remote Sensing of Environment* 117: 72–82. doi:[10.1016/j.rse.2011.07.020](https://doi.org/10.1016/j.rse.2011.07.020).